

Ground-state and low-lying excitations of the periodic Anderson Hamiltonian in one dimension from finite-cell calculations

R. Jullien and Richard M. Martin*

Laboratoire de Physique des Solides, Université Paris-Sud, F-91405 Orsay, France

(Received 18 June 1982)

We present the calculations of the ground state and lowest excited states of the one-dimensional periodic Anderson Hamiltonian with two electrons per site and arbitrary magnitude of the repulsive interaction U . We consider finite cells (up to $N=4$) and introduce a new method, using modified periodic boundary conditions, to facilitate comparison of calculations with different N . The ground state is found to be a nonmagnetic singlet in all cases. The lowest-energy excitations for adding or subtracting one electron show that the system is insulating and the lowest spin-flip excitations indicate a near instability to antiferromagnetism due to the "nesting" of the Fermi surface in one dimension. The lowest excitations are shown to vary little with N and, for $N=4$, the results agree well with infinite-cell calculations, both for small U and for the Kondo-lattice regime. The primary results are the continuous variation from $U=0$ to the Kondo-lattice and mixed-valence regimes and the importance of correlations, which lead to the insulating gap and dispersion in the electronic and spin excitations.

I. INTRODUCTION

The physics of anomalous rare-earth elements and compounds is the subject of increasing theoretical interest.^{1,2} Their properties, such as mixed-valence and Kondo effects, are caused by the presence of a narrow band of strongly correlated f electrons lying in the vicinity of the Fermi surface. Some aspects of these problems can be explained within impurity theories,³⁻⁶ which consider the rare-earth compound as a collection of independent f -impurity levels described by the Anderson impurity Hamiltonian. In addition, however, there are collective effects that are unique to a periodic lattice⁷⁻¹⁰ and cannot be described at all by an assembly of impurities. The periodic Anderson Hamiltonian which contains the coherence effects appears to be the most appropriate Hamiltonian able to describe the important features of anomalous rare-earth crystals. To our knowledge, this Hamiltonian has been only studied up to now only within the Hartree-Fock approximation,¹¹ perturbation expansion in the interaction,¹² variational approaches,^{13,14} Green's-function truncation methods,^{15,16} the "alloy" coherent-potential approximation (CPA),^{9,17} and limited calculations on finite cells.¹⁸ The central issue which has arisen is whether the ground state is a nonmagnetic singlet with an insulating gap^{7-11,13,17} or a metal.¹⁴⁻¹⁶ None of these methods is complete for large U and, in fact, each is

known to be unable to describe the Kondo effect, even qualitatively. Therefore, it is essential to address the central issues of this problem and to examine the full range from mixed-valence to the Kondo regime, which has been studied independently as a "Kondo lattice."^{7,8} Furthermore, the existence of the insulating gap in this special case is significant for more general cases because the gap is one aspect of a Fermi-liquid formulation of Fermi-surface properties with implications for many systems, insulating and metallic.^{9,10}

Here we present exact calculations done on finite cells, taking into account correlations in all regimes (including mixed-valence and Kondo). Because of the complexity of the many-body problem, only small cells (up to $N=4$) can be treated exactly. For that reason we present a new method, modified periodic boundary conditions, to improve the extrapolation to large cells ($N \rightarrow \infty$). Portions of this work have been described in previous short papers.¹⁹ The outline of this paper is as follows. In Sec. II we present the Hamiltonian, give its diagonalization for trivial limiting cases, and discuss essential properties of the ground state using the impurity Kondo problem as a guide. The methodology of the numerical calculations for finite cells is given in Sec. III. In Secs. IV and V we present the results for the lowest-energy electronic and magnetic excitations of the interacting electron problem. In Sec. VI we discuss the results and the

implications for the properties of infinite Anderson lattices.

II. MODEL

A. Anderson lattice Hamiltonian

The periodic Anderson Hamiltonian is the extension of the original one-impurity Anderson Hamiltonian²⁰ to the concentrated case of rare-earth atoms regularly spaced on each site of a lattice. Let us write generally

$$\mathcal{H} = H - \mu N_p, \quad (1)$$

where \mathcal{H} and H represent the Hamiltonian per site, respectively, in the grand canonical and canonical representation, μ is the Fermi energy (or chemical potential), and N_p is the total number of particles per site. For a one-dimensional lattice and using the k -space notations, the Hamiltonians can be written

$$\begin{aligned} H = & \sum_{k,\sigma} [\epsilon_f f_{k\sigma}^\dagger f_{k\sigma} + t \cos k d_{k\sigma}^\dagger d_{k\sigma} \\ & + V(d_{k\sigma}^\dagger f_{k\sigma} + f_{k\sigma}^\dagger d_{k\sigma})] \\ & + (U/N) \sum_{k_1 k_2 k_3} f_{k_1 \uparrow}^\dagger f_{k_2 \uparrow} f_{k_3 \uparrow}^\dagger f_{(k_1+k_2-k_3) \downarrow}, \end{aligned} \quad (2)$$

with

$$N_p = \sum_{k,\sigma} (d_{k\sigma}^\dagger d_{k\sigma} + f_{k\sigma}^\dagger f_{k\sigma}), \quad (3)$$

where $f_{k\sigma}^\dagger$ ($f_{k\sigma}$) and $d_{k\sigma}^\dagger$ ($d_{k\sigma}$) are creation (destruction) operators for electrons in the f band and d band, respectively, with wave vector k and spin σ .

The broad d band is centered at energy $\epsilon_d=0$ and chosen to have the symmetric nearest-neighbor cosine form. The f band is centered at energy ϵ_f , V is a constant hybridization parameter between the two bands, and U is the Coulomb repulsion in the f band. The summation on \vec{k} is restricted to the N possible values of \vec{k} , N being the number of sites of the lattice. With regular periodic boundary conditions, these values are $k = 2n\pi/N$, $n = 1, \dots, N-1, N$. The summation on σ is restricted to the two possible values $\sigma = +1$ or -1 (\uparrow or \downarrow). Both bands are only spin degenerate, and orbital degeneracies are completely neglected. This is the primary restriction which does not allow Eq. (2) to describe all the detailed effects which are different for each type of rare-earth ion. However, it is well known that, apart from this restriction, the Hamiltonian describes the main physical situations of anomalous rare-earth compounds including the Kondo effect

and the mixed-valence regime. The Kondo effect occurs when the atomic f energies ϵ_f and $\epsilon_f + U$ are both far away from the Fermi level μ and the mixed-valence regime occurs when ϵ_f (or $\epsilon_f + U$) is near μ . Before presenting our calculations, let us discuss some simple limits where the Hamiltonian can be solved exactly in the $N \rightarrow \infty$ case.

B. The $U=0$ limit

When there are no electron-electron interactions, i.e., when $U=0$, the Hamiltonian is easily diagonalized. The system is described by two hybridized subbands $\epsilon_0^+(k)$ and $\epsilon_0^-(k)$ with dispersion relations

$$\begin{aligned} \epsilon_0^\pm(k) = & \frac{1}{2}(t \cos k + \epsilon_f) \\ & \pm \frac{1}{2}[(t \cos k - \epsilon_f)^2 + 4V^2]^{1/2}. \end{aligned} \quad (4)$$

The main features of that band structure is the existence of a nonzero indirect energy gap, with ϵ_f in the gap, and a narrow resonance near the gap edges due to the small dispersion of $\epsilon_0^\pm(k)$ near ϵ_f . The indirect energy gap (between $k=0$ and $k=\pi$) is given by

$$G_{0\pi} = (t^2 + 4V^2)^{1/2} - t \approx 2V^2/t = \Delta, \quad (5)$$

when $\epsilon_f=0$ and V is small. The parameter Δ also measures the width of the resonance near the gap edges. These qualitative features as well as the order of magnitude of the gap and the resonance width are not affected by varying ϵ_f in the band, except near the band edges. These well-known results can be contrasted with the one-impurity case, where there is also a resonance of width Δ at ϵ_f , the so-called Friedel-Anderson virtual-bound-state (VBS) resonance. The essential difference is the existence of a gap within the resonance in the periodic case resulting from the coherent hybridization between the d and f bands.

A physical situation of particular interest, which will be considered throughout this paper, is the case where $N_p = 2N$. Then the ground state for $U=0$ has a filled lower subband and the system is insulating, with a gap $\sim \Delta$ caused by the hybridization V . One important problem, which is a motivation for this study, is to know if this insulating phase remains stable in presence of strong electron-electron interactions.

C. The interacting cases: $U \neq 0$

In cases with large interactions U , it is instructive to consider the isolated ion limit where $V=0$. Then

H separates into f and d parts that can be diagonalized separately in real space and k space, respectively. The f part leads to a system of independent f ions on each site. The energy is 0, ϵ_f , or $2\epsilon_f + U$ if the site is unoccupied, occupied by one f electron, or occupied by two f electrons, respectively. First, consider $\epsilon_f < 0$ and $\epsilon_f + U > 0$, in which case the lowest-energy states have one f electron on each site and the d band is half occupied. The ground state is magnetically degenerate (the f electrons with spin either up or down) and metallic (the d band is partially filled). If $\epsilon_f > 0$ in the upper half of the d band (or $\epsilon_f + U < 0$ in the lower half), there is fractional f occupation, i.e., mixed valence, where the lowest-energy state is degenerate with respect to the sites of ions of different valence as well as the magnetic configuration.

In order to derive a unique ground state, it is essential to include a nonzero hybridization V . This completely changes the nature of the solution, as is well known from impurity problems.²¹ In the one-impurity case, exact solutions of the Kondo²² and Anderson²³ problems have now shown that the hybridization leads to a nonmagnetic singlet ground state in all cases. This is best known in the Kondo regime, where Schrieffer and Wolff²⁴ showed that the Anderson Hamiltonian transforms into the Kondo Hamiltonian with antiferromagnetic coupling between the spin of the localized f electron and the spins of the conduction electrons:

$$H_K = \sum_{k,\sigma} \epsilon_k d_{k\sigma}^\dagger d_{k\sigma} + (J/N) \sum_{k,k'} [2(S_n^+ d_{k\downarrow}^\dagger d_{k'\uparrow} + S_n^- d_{k\uparrow}^\dagger d_{k'\downarrow}) + S_n^z (d_{k\uparrow}^\dagger d_{k'\uparrow} - d_{k\downarrow}^\dagger d_{k'\downarrow})] \times \exp[i(k - k')n], \quad (6)$$

where n is the impurity site and the f spin is represented by the Pauli matrices. In the one-dimensional case the Schrieffer-Wolff (SW) formula is

$$J \simeq V^2 (1/|\epsilon_f| + 1/|\epsilon_f + U|), \quad (7)$$

which reduces to $J \simeq 4V^2/U$ in the symmetrical case. The electrons at the Fermi energy are greatly affected with a phase shift of $\pi/2$, the maximum allowed by the unitarity limit. This is due to the information of a many-body Kondo resonance²¹ at the Fermi level of width

$$T_K \sim t \exp(-t/J). \quad (8)$$

The Kondo resonance at the Fermi level, which be-

comes very narrow when the f level is far away from the Fermi surface, is distinct from the VBS resonance of width Δ which occurs in the vicinity of the f levels. The singlet ground state develops continuously to the mixed-valence regime, where the Kondo and VBS resonances merge and lose their distinct identity.^{3-6,23}

The subject of this paper is the nature of the ground state and the lowest-energy excitations in the case of a lattice of f states. Just as in the impurity case, the hybridization V is the essential ingredient to lift the degeneracy and determine the ground state. We report exact results for finite periodic cells for $V \neq 0$, arbitrary values of $U > 0$, and all situations including the Kondo and the mixed-valence regimes. Note, in particular, that we study the "Kondo-lattice effect" by starting directly from the periodic Anderson Hamiltonian without assuming the SW transformation. There is at present no derivation of the SW transformation in the periodic case,²⁵ therefore the present calculations give results which are independent of previous work using the Kondo-lattice Hamiltonian,^{7,8,25-28} which is the generalization of (6) to a periodic lattice of f spins.

III. METHODS

A. The modified periodic boundary conditions

In this paper we consider finite one-dimensional cells of N sites (labeled $n = 1, 2, \dots, N$) closed into a ring. Each cell is invariant under the N finite rotations which transform site n into site $n + \Delta n$. This invariance leads to conservation of momentum, so that the many-body states are eigenstates of k satisfying the Bloch condition

$$\psi_n = \psi_k e^{ikn}, \quad (9)$$

and the boundary condition

$$\psi_N \equiv \psi_0 \quad (10)$$

is equivalent to the Born-von Kármán periodic boundary condition

$$k = 2m\pi/N, \quad (11)$$

where the integers m define N points within the one-dimensional Brillouin zone $-\pi < k \leq \pi$.

Our purpose is to carry out exact calculations for different N and to draw conclusions relevant to the limit $N \rightarrow \infty$. However, it is apparent that the properties may vary in a nonmonotonic way with

N . In particular, the k states that are closest to the Fermi surface are most important in the ground state of the interacting system; however, the relation of the points in each finite set to the Fermi surface varies with N . Let us denote by k_F the Fermi wave vector in the thermodynamic limit (i.e., when $N \rightarrow \infty$). There is no special reason that k_F should be included in the set of k points for every finite cell of size N . For example, when the Fermi energy is at the center of the d band, $k_F = \pm\pi/2$ for the decoupled d band, and the values $\pm\pi/2$ are included in the set of k points only for $N=4, 8, 12$, etc. When f - d coupling is introduced, all the ground-state properties will thus vary with N with oscillations of period 4. This makes impossible any direct extrapolation to $N \rightarrow \infty$ by comparing only a few small cells.

To improve this situation we have introduced "modified" periodic boundary conditions including an arbitrary phase φ :

$$\psi_N \equiv \psi_0 e^{i\varphi}. \quad (12)$$

This leads to

$$k = 2n\pi/N + \varphi/N, \quad (13)$$

so that by choosing φ any k point can be reached. This is illustrated in Fig. 1 in the case of a simple cosine band. The same set of k points is recovered when φ is increased by $2\pi/N$ so that each ground-state property varies with φ with period $2\pi/N$. The "best" results are obtained when φ is chosen so that k_F is included in the set of k 's for each finite cell. For this particular choice of φ , different size cells can be best compared and the oscillations with N are broken. In the example where $k_F = \pi/2$, we

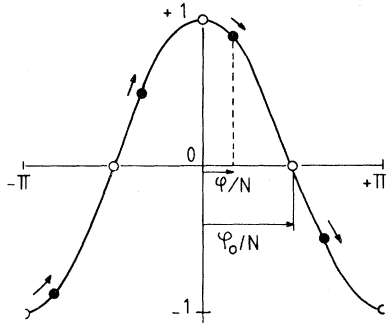


FIG. 1. Energy of noninteracting states of a finite cell with $N=4$, as a function of k defined by the modified periodic boundary conditions. The phase φ shifts each k in the finite set by φ/N , as in Eq. (14). The optimum phase $\varphi = \varphi_0$ is that for which the Fermi wave vector of the infinite system, k_F , is included in the set of k points.

choose

$$\varphi = \varphi_0(N) = N\pi/2. \quad (14)$$

There remains a simple odd-even alternation coming from the fact that for N odd only $k_F = \pi/2$ is reached while for N even both $k_F = \pi/2$ and $k_F = -\pi/2$ are included. Here we concentrate upon even values of N , where Eq. (14) corresponds to regular periodic conditions ($\varphi_0 = 0$) for $N/2$ even and "antiperiodic" boundary conditions ($\varphi_0 = \pi$) for $N/2$ odd. This method has been systematically used on a simpler interacting fermion Hamiltonian (for which larger cells could be treated) and the extrapolation to $N \rightarrow \infty$ was greatly facilitated.²⁹ Here we are more modest since the complications of the Hamiltonian limit us to $N \leq 4$. The only direct comparison is between the results for $N=2$ with $\varphi = \pi$ and $N=4$ with $\varphi = 0$.

B. Principles of the calculation: Ground state

The exact diagonalization of H is performed by diagonalizing its representative matrix in each subspace corresponding to a choice of φ and to the possible values of the following quantum numbers which commute with H : the projection of the total spin on the z axis,

$$\Sigma^z = \sum_k (d_{k\uparrow}^\dagger d_{k\uparrow} - d_{k\downarrow}^\dagger d_{k\downarrow} + f_{k\uparrow}^\dagger f_{k\uparrow} - f_{k\downarrow}^\dagger f_{k\downarrow}), \quad (15)$$

the total number of electrons N_p given by (3), and the total wave vector K . We have first determined the absolute ground state of H for $N_p = 2N$ with energy E_{2N}^0 , spin Σ^{0z} , and total wave vector K^0 . This determination has been performed by using the Lanczös procedure,³⁰ which greatly reduces the size of the matrix to be diagonalized (for $N=4$ and $N_p=8$, the original matrix is of order 1236).

In the Lanczös algorithm one starts from a trial normalized vector ψ_1 on which H is applied,

$$H\psi_1 = \alpha_1\psi_1 + \beta_1\psi_2, \quad (16)$$

where α_1 and β_1 are determined unambiguously such that ψ_2 is normalized and orthogonal to ψ_1 . The procedure is repeated on ψ_2 , etc., up to step n , where

$$H\psi_n = \dots + \delta_{n-2}\psi_{n-2} + \gamma_{n-1}\psi_{n-1} + \alpha_n\psi_n + \beta_n\psi_{n+1}, \quad (17)$$

where ψ_{n+1} is normalized and orthogonal to

ψ_1, \dots, ψ_n . The fact that H is symmetric implies many simplifications: All the coefficients in (17) are zero except α , β , and the γ 's, and, furthermore, $\beta_n \equiv \gamma_n$. Finally (17) reduces to

$$H\psi_n = \beta_{n-1}\psi_{n-1} + \alpha_n\psi_n + \beta_n\psi_{n+1}. \quad (18)$$

In the basis $\{\psi_n\}$, H is represented by a tridiagonal symmetric matrix. At each step the tridiagonal matrix is determined and diagonalized by a standard subroutine. In the present problem we find that after approximately 20 Lanczös steps the ground-state energy is obtained within 10^{-7} accuracy.

The trial starting vector has been chosen of the form

$$\psi_1 = d_{k_1, \sigma_1}^\dagger \cdots d_{k_p, \sigma_p}^\dagger f_{k_{p+1}, \sigma_{p+1}}^\dagger \cdots f_{k_q, \sigma_q}^\dagger |0\rangle, \quad (19)$$

where a product of N_p different creation operators has been considered with the conditions

$$\sum_{i=1}^q k_i = K, \quad \sum_{i=1}^q \sigma_i = \Sigma^z. \quad (20)$$

For $N_p = 2N$, we have tried several trial starting vectors corresponding to all possible values of K and Σ^z and we have always observed that the absolute ground state can be generated by the starting vector representing a filled d band,

$$\psi_1^0 = \prod_{k, \sigma} d_{k\sigma}^\dagger |0\rangle, \quad (21)$$

where the product contains the N different k points and the two possible values of σ . Thus the ground state for $N_p = 2N$ is a nonmagnetic singlet with $\Sigma^z = 0$ and $K = K^0$ given by

$$\begin{aligned} K^0 &= \sum k_m = \sum (2m\pi/N + \varphi/N) \\ &= \begin{cases} \varphi & \text{for } N \text{ even} \\ -\pi + \varphi & \text{for } N \text{ odd} \end{cases}. \end{aligned} \quad (22)$$

Furthermore, the exact ground state is an analytic continuation of the $U=0$ state, generated by mixing higher-order electron-hole excitations with no change in the analytic character or crossing of states. We have calculated the ground-state energy E_{2N}^0 and we have verified that it is a periodic function of φ with period $2\pi/N$. The ground state thus determined, we then proceed to find the low-energy excitations from the ground state.

C. Electronic and magnetic excitations

In order to determine the excitation energies for adding one electron, we have determined the

ground-state energy of H for $N_p = 2N + 1$ and $K = K^0 + k$ by using the trial starting vector

$$\psi_1 = f_{k\sigma}^\dagger \psi_1^0. \quad (23)$$

The same result is obviously obtained for $\sigma = \pm 1$, so that this excited state is magnetically doubly degenerate. The ground-state energy found in the subspace is denoted $E_{2N+1}(k)$ and is calculated with the same φ value as for E_{2N}^0 . Then we define

$$\epsilon^+(k) = E_{2N+1}(k) - E_{2N}^0. \quad (24)$$

In fact the definition of the one-electron excitation energy involves the eigenvalues of \mathcal{H} instead of H , and is given by

$$\mathcal{E}_{2N+1}(k) - \mathcal{E}_{2N}^0 = \epsilon^+(k) - \mu. \quad (25)$$

Thus $\epsilon^+(k)$ represents the one-electron excitation shifted by μ . Similarly, we have determined the hole excitation energy,

$$\mathcal{E}_{2N}^0 - \mathcal{E}_{2N-1}(k) = \epsilon^-(k) - \mu, \quad (26)$$

with

$$\epsilon^-(k) = E_{2N}^0 - E_{2N-1}(k), \quad (27)$$

by determining the ground-state energy $E_{2N-1}(k)$ of H for $N_p = 2N - 1$ and $K = K^0 - k$, using the trial starting state

$$\psi_1 = d_{k\sigma} \psi_1^0. \quad (28)$$

The electronic excitations can be also conveniently described in terms of electronic gap

$$\begin{aligned} G_{kk'}^{\text{el}} &= \epsilon^+(k') - \epsilon^-(k) \\ &= E_{2N+1}(k') + E_{2N-1}(k) - 2E_{2N}^0. \end{aligned} \quad (29)$$

These gaps define the difference in the energies required to extract an electron of wave vector k and to add an electron at wave vector k' .

By varying φ , any k value can be reached and continuous curves $\epsilon^\pm(k)$ can be drawn. When there is no interaction, the variations of E_{2N}^0 and $E_{2N\pm 1}(k)$ with φ cancel and we recover the single-electron and -hole curves exactly (except some special effect which will be described in Sec. IV A). In the presence of electron-electron interactions, there are artificial oscillations in $\epsilon^\pm(k)$ of period $2\pi/N$ with best results for the set of k points that correspond to $\varphi = \varphi_0$. These oscillations are much more pronounced if there is a large dispersion of the points from which is constructed the resulting many-body state. In principle, these artificial oscillations must disappear in the large- N limit where $\epsilon^\pm(k)$ must reproduce the exact electron and hole

dispersion curves of the infinite system.

It is also interesting to determine the magnetic excitations from the $N_p=2N$ ground state. Each excitation can be found by two independent calculations. On the one hand, one can determine the ground-state energy $E_{2N}^1(k)$ in the subspace with the quantum numbers

$$N_p=2N, \quad \Sigma^z=\pm 2, \quad K=K^0+k. \quad (30)$$

On the other hand, one can calculate the first excited state in the subspace $N_p=2N$, $\Sigma^z=0$, $K=K^0+k$. We have checked that these three states, with $\Sigma^z=+2, 0, -2$, form a degenerate triplet as expected from the general property of spin-rotation invariance of H . The ground state for Eq. (30) is determined by starting with the following trial function:

$$\psi_1 = d_{k_1 \uparrow} f_{(k_1+k) \downarrow}^\dagger \psi_1^0. \quad (31)$$

The result is independent of k_1 and we define the magnetic excitation spectrum by

$$G_k^{\text{mag}} = E_{2N}^1(k) - E_{2N}^0. \quad (32)$$

As introduced in (32), k is necessarily of the form $2n\pi/N$ and cannot reach any value by varying φ . So we can calculate only N gaps G_k^{mag} , each gap being a periodic function of φ with period $2\pi/N$, and we cannot draw a continuous curve as in the case of the electronic excitations $\epsilon^\pm(k)$. The electronic and magnetic gaps have the same magnitudes when there is no electron-electron interaction, so that we must recover

$$G_{kk'}^{\text{el}} = G_{k'-k}^{\text{mag}} \quad \text{for } U \rightarrow 0, \quad (33)$$

except for cases in which the triplet states are forbidden. These exceptional cases have an important role in finite cells as we shall see in Sec. V. When finite interactions are introduced, this equality does not hold and it is interesting to study the different excitation gaps independently.

IV. RESULTS FOR THE ELECTRONIC EXCITATIONS

A. Small- U limit

In principle, as explained in Sec. III C, our method must give the analytic result of Sec. II B when $U \rightarrow 0$. In fact, we observe that there is an apparent discontinuity between the analytic results valid for $U=0$ and the limit $U \rightarrow 0$. This is due to the fact that in the presence of the U -term (even if

U is infinitesimal) states far from the Fermi level can decay by excitation of electron-hole pairs. This mechanism can be compared with the Auger effect. It can occur here because of the special band shape when $U=0$. The excitation energy $\epsilon^+(k)$ for $U=0$ is obtained from the ground state $N_p=2N$ by putting the extra electron at wave vector k in the upper subband which is completely empty; this is the energy $\epsilon_0^+(k)$ given by (4). However, for $U \neq 0$, the presence of the four-operator term allows us in some cases to reach a lower energy by putting instead two electrons at wave vectors k_1 and k_2 in the upper band and a hole at k_1+k_2-k in the lower band. Thus, for U , infinitesimal $\epsilon^+(k)$ is given by

$$\epsilon^+(k) = \min[\epsilon_0^+(k), \epsilon_0^+(k_1) + \epsilon_0^+(k_2) - \epsilon_0^-(k_1+k_2-k)], \quad (34)$$

where the right-hand side means the minimum considering all allowed k_1 and k_2 . For example, in the case of $\epsilon_f=0$, adding an electron in the upper subband at $k=0$ costs energy $\sim t$, whereas adding two electrons (of opposite spins) at $k_1=k_2=\pi$ and a hole at $k=-k_1-k_2=0$ costs energy $2\epsilon_0^+(\pi) - \epsilon_0^-(0) \simeq 2V^2/t$. For finite cells only few k points are available in that the reduction of $\epsilon^+(k)$ cannot be as complete as for $N \rightarrow \infty$. This is quantitatively shown for $\epsilon_f=0$ in Fig. 2 where we have represented by full curves the result obtained for $\epsilon^+(k)$ when it does not coincide with $\epsilon_0^+(k)$. In the infinite-system limit the physical meaning of $\epsilon^+(k)$ is basically different when it corresponds to $\epsilon_0^+(k)$ or when it corresponds to a many-body excitation. When $\epsilon^+(k)$ corresponds to $\epsilon_0^+(k)$ one can speak of a single-electron excitation well separated (by a gap) from the continuum of other excitations. When

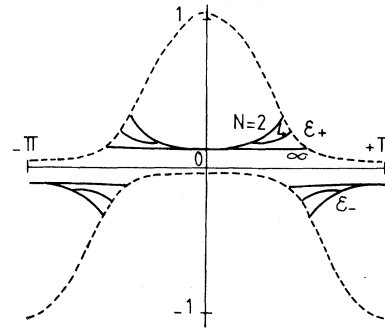


FIG. 2. Lower limits of the electron (hole) excitations for $U \rightarrow 0$ as a function of k (i.e., φ) for different N . The results are shown as solid curves where they differ from the dashed curves, which are the one-electron eigenstates for $U=0$.

$\epsilon^+(k)$ is the result of an Auger-type mechanism it is the bottom of a continuum of one-electron excitations. For finite cells the continuum is not formed so that in our calculations one cannot really distinguish between the two situations.

When $V \ll t$ there results a very flat band with dispersion of order $\Delta = 2V^2/t$. The lowest gap is not changed by this mechanism and remains the indirect $0 \rightarrow \pi$ gap, $G_{0\pi}^{\text{el}} \simeq 2V^2/t = \Delta$. However, the lowest direct gap changes from $G_{\pi/2, \pi/2}^{\text{el}} = 2V$ for $U=0$ to $G_{00}^{\text{el}} = G_{\pi, \pi}^{\text{el}} \simeq 2\Delta$. Note that the direct gap at $\pi/2$, $G_{\pi/2, \pi/2}^{\text{el}}$, is not reduced for $N=4$, while it is reduced in the infinite-lattice case

B. Kondo-lattice regime

Here we present the results obtained for large U in the electron-hole-symmetric case where $\epsilon_f = -U/2$, $N_p = 2N$, and μ is zero by symmetry. The electronic excitation energies $\epsilon^\pm(k)$ are given in Fig. 3 for $U = 1.5t$, $V = 0.2t$, and even $N=2$ and 4. Note that the electron-hole symmetry is recovered by the fact that $\epsilon^+(k) = \epsilon^-(\pi - k)$. In each case φ has been varied so that each k is reached. As expected from the discussion of Sec. III C, the curves are affected by large artificial oscillations of period $2\pi/N$ that is due to the large dispersion of the d states from which are constructed the resulting many-body states. We have represented by dots the best set of points in each case, i.e., corresponding to $\varphi = \varphi_0(N)$. When going from $N=2$ to $N=4$, one observes clearly the doubling of the period and the decrease, by almost a factor of 2, of the amplitude of the oscillations. The four best points for $N=4$ have a very flat dispersion and the corresponding excitation energies are comparable to that of the two best points for $N=2$. When $N \rightarrow \infty$, one could expect a finite gap with very flat electronic and hole dispersions near the edge of the gap. This very

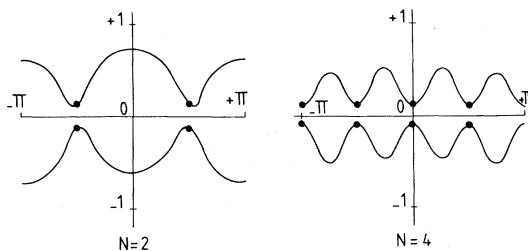


FIG. 3. Lower limits of the electronic excitation spectrum as a function of k in the symmetric Kondo-lattice case with $\epsilon_f = -U/2$, $U = 1.5t$, $V = 0.2t$, and $N = 2$ and 4.

small dispersion must be attributed to the formation of a narrow many-body resonance due to the Kondo effect, as occurs in the Kondo-impurity problem.

The same calculations have been done for several values of U . To summarize the results we have reported the electronic gaps (best points) obtained for $N=4$ as a function of U in Fig. 4. We recall that increasing U corresponds to decreasing ϵ_f simultaneously such that $\epsilon_f = -U/2$. For small U the gaps $G_{0\pi}^{\text{el}}$ and $G_{\pi/2, \pi/2}^{\text{el}}$ vary as U^2 with coefficients which are respectively positive and negative. This agrees well with recent perturbation expansions in U done by Yamada and Yoshida¹² for the infinite ($N \rightarrow \infty$) one-dimensional Anderson lattice. In order to compare quantitatively we have shown the parabolas corresponding to their U^2 terms by dashed curves and we can observe that the agreement is remarkably good. For large U all the gaps converge to the same asymptotic curve which scales like V^2/U . More quantitatively this asymptotic behavior is estimated to be

$$G^{\text{el}} \underset{U \rightarrow \infty}{\sim} 7V^2/U. \quad (35)$$

From Eq. (35) the electronic gap scales as the Kondo coupling constant $J = 4V^2/U$ when $J \rightarrow 0$. This agrees well with finite-cell calculations done directly on the Kondo-lattice Hamiltonian,²¹ where it has been found that the electronic gap scales as J while the magnetic gap scales as J^2 for $J \rightarrow 0$. The results for the electronic gap are also comparable with renormalization-group (RG) calculations done directly on the Kondo-lattice Hamiltonian.²⁸ The charge gap obtained with the three-site blocking method of Ref. 7 is reported by a dashed line in Fig. 4. The agreement is perhaps fortuitous because the RG method of Ref. 7 gives a result only slightly

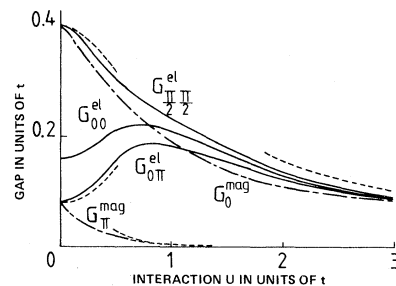


FIG. 4. Electronic gaps G^{el} (solid lines) and magnetic gaps G^{mag} (dotted-dashed lines) as a function of U in the symmetric Kondo-lattice case with $\epsilon_f = -U/2$, $V = 0.2t$, and $N = 4$. Dashed lines give perturbation results for $N = \infty$ from Ref. 12, and Kondo-lattice results from Ref. 7 using Eq. (7) for J .

lowered by renormalization below the finite cells result for $N=3$ (without periodic boundary conditions). More recent RG calculations²⁷ show that the gap varies as $\exp(-1/J)$ when $J \rightarrow 0$ but no quantitative curve for the gap has been drawn. This improved result would be lower than the U^{-1} behavior obtained here for finite cells. However, we cannot hope to recover the exponential behavior $T_k \sim \exp(-1/J)$ for finite cells. This behavior must be only asymptotically recovered in the limit $N \rightarrow \infty$.

C. Mixed-valence regime

We present now corresponding results in a mixed-valence case. The energies $\epsilon^\pm(k)$ are given in Fig. 5 for $U=1.5t$, $V=0.2$, and $\epsilon_f=0$. With this choice of ϵ_f , the lower f level is near the Fermi energy while the other one (at ϵ_f+U) is far above. Here, also we discuss only the curves obtained for $N=2$ and 4. Note that there is always a gap but now we must choose $\mu > 0$ (in the gap) if there are exactly two electrons per site. This means that the f level has been effectively shifted, as found in Hartree-Fock¹¹ and CPA (Refs. 9 and 17) calculations so that ϵ_f is not in the gap. We observe a great difference between electrons and holes. The hole dispersion curve depends little on N and looks like the simple $U \simeq 0$ curve shown in Fig. 2, while the electron dispersion curve shows the same artificial oscillations of period $2\pi/N$ in k as in the Kondo case. We think that the artificial oscillations are present in both cases; however, in the hole case their amplitude is smaller since the many-body states are formed from less dispersive states, the f level being just below the Fermi level. Another important difference from the Kondo regime is the dispersion of the best points. The gaps for $N=4$ have been plotted in Fig. 6, and one can see that they do not vary much with U and they tend to constant values

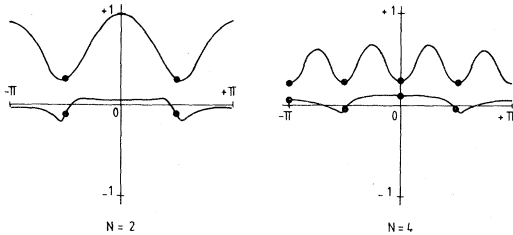


FIG. 5. Electronic excitation spectrum in a mixed-valence case where $\epsilon_f=0$, $U=1.5t$, $V=0.2t$, and $N=2$ and 4.

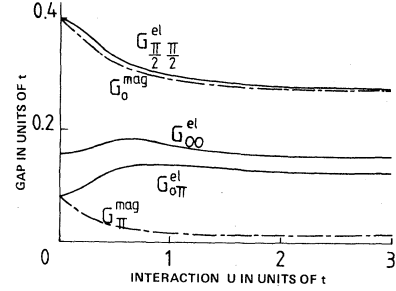


FIG. 6. Electronic gaps as a function of U in a mixed-valence case where $\epsilon_f=0$, $V=0.2t$, and $N=4$.

of order Δ when $U \rightarrow \infty$. The minimum electronic gap is actually *increased* above the $U=0$ case. This gives strong support to previous conclusions^{7-11,13,17} that a gap $\sim \Delta$ remains even in the presence of strong electron interactions $U \gg \Delta$.

D. Continuity between the regimes

We have completed our study of electronic excitations by varying ϵ_f from $-U/2$ up to values of order $\pm\Delta$, keeping U fixed, in order to see the crossover when coming from the Kondo-lattice regime to the mixed-valence regime. As expected, the crossover arises when ϵ_f becomes of order $-\Delta$. There is complete continuity for the gap and the electronic dispersion when ϵ_f varies. This is illustrated in Fig. 7 where, for $U=1.5t$ and $V=0.2t$, we have plotted representative measures of the electronic and hole dispersion defined by

$$\delta_e = \epsilon^+(0) - \epsilon^+(\pi) \quad (36)$$

and

$$\delta_h = \epsilon^-(0) - \epsilon^-(\pi). \quad (37)$$

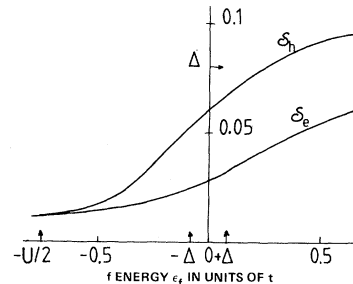


FIG. 7. Dispersion of the lowest-energy electron and hole excitations δ_e and δ_h defined in Eqs. (36) and (37) as a function of ϵ_f for $U=1.5t$, $V=0.2t$, and $N=4$.

One can observe the crossover between widths smaller than Δ in the Kondo-lattice regime to values of order Δ in the mixed-valence regime. Note that the resonance width for the holes remain always larger than the resonance for the electrons indicating as asymmetric resonance around the gap. Obviously, for ϵ_f smaller than $-U/2$, electrons and holes are interchanged and the crossover arises when $\epsilon_f + U \approx \Delta$.

V. RESULTS FOR THE MAGNETIC EXCITATIONS

A. Small- U limit

For $\epsilon_f=0$ and $U=0$ the dispersion relation for the magnetic gap in the infinite lattice is

$$G_k^{\text{mag}} = [t^2 \sin^2(k/2) + 4V^2]^{1/2} - t \sin(k/2), \quad (38)$$

which is given by the full curve in Fig. 8. For finite cells of size N , there are N gaps $G_k^{\text{mag}}, k=2n\pi/N$, each of which is a periodic function of φ even for $U=0$. The value given by (38) is exactly recovered only for special values of φ for which G_k^{mag} is minimum. This is illustrated in Fig. 9 where we have plotted G_k^{mag} as a function of φ for $U=0$ for two values of k ($k=0$ and π) and for $N=2, 4$, and 8 . One can see how the oscillations with φ decrease when N increases and how $G_k^{\text{mag}}(\varphi)$ reaches its minimum value which corresponds exactly to for-

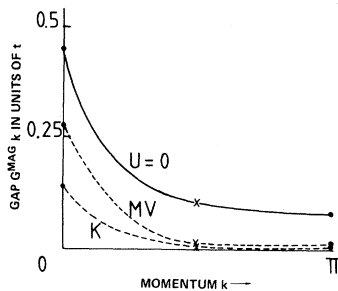


FIG. 8. Dispersion of the magnetic gap G_k^{mag} . The solid curve for $U=0$ is given analytically by formula (38). The other curves (dashed curves) correspond to the Kondo case (K) and mixed-valence case (MV), with $\epsilon_f = -U/2$ and $\epsilon_f = 0$, respectively, and $U=1.5t$, $V=0.2t$, and $N=4$. Only the three points for $k=0$, $\pi/2$, and π are known (they correspond to the best points of Figs. 10 and 11) and the dashed curves have been drawn as a guide to the eye.

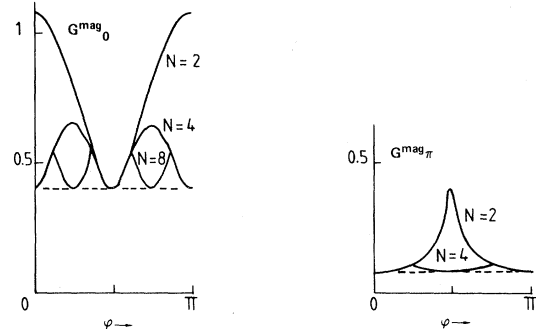


FIG. 9. Magnetic gaps G_0^{mag} and G_π^{mag} as a function of φ in the noninteracting case $U=0$ for $V=0.2t$ and $N=2, 4$, and 8 . The dashed curves correspond to the exact result for $N \rightarrow \infty$.

mula (38) (dashed lines in Fig. 1). For $N=4$ the exact value is recovered for $\varphi=0$ [which is the value of $\varphi, \varphi=\varphi_0(N)$, which gives also the best values for the electronic gap], while for $G_\pi^{\text{mag}}(\varphi)$ (not shown) the exact value is recovered for $\varphi=\pi/4$.

For $U \rightarrow 0$ there is a potential reduction in the magnetic gaps by many-particle excitations just as for the electronic gaps. The lowest gap is given by Eq. (34); however, for triplet magnetic excitations we must add the condition $k_1 \neq k_2$ because of the Pauli exclusion principle for electrons of the same spin. This turns out to be an essential difference in the small cells with $N \leq 4$, so that in these cases there is no reduction of the lowest magnetic gap at any k . For larger cells there exists a triplet excitation with energy only slightly above the singlet, and for $N \rightarrow \infty$ the magnetic and electronic gaps must approach the same value. This shows that the dispersion of the magnetic gaps found for $N \leq 4$ is not representative of large cells. Nevertheless, we can get very useful information from the small cells. In particular, for large U the minimum magnetic and electronic gaps, both at $k=\pi/2$, can be compared and we can find the relative sizes of the gaps in the Kondo and mixed-valence regimes.

B. Kondo-lattice regime

The results for G_0^{mag} and G_π^{mag} as a function of φ for $N=2$ and 4 are reported in Fig. 10 for the Kondo-lattice set of parameters of Sec. IVB: $\epsilon_f = -U/2$, $U=1.5t$, and $V=0.2t$. One observes the same kind of oscillations with φ as for $U=0$ and the best values can be estimated from the minimums of these curves. The best points have been reported as a function of k in Fig. 8 where

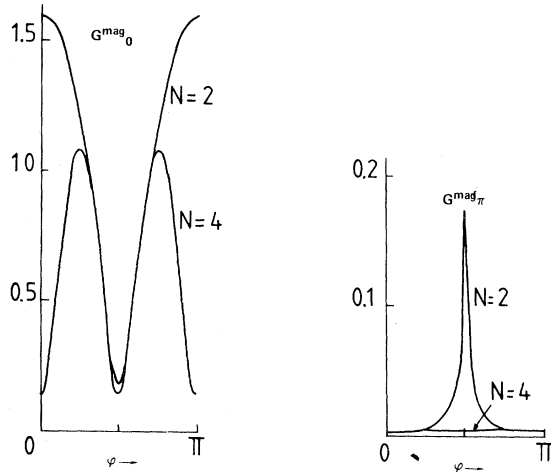


FIG. 10. Magnetic gaps G_0^{mag} and G_π^{mag} as a function of φ in the Kondo-lattice case for $\epsilon_f = -U/2$, $U = 1.5t$, $V = 0.2t$, and $N = 2$ and 4 .

they can be compared with the $U = 0$ results. The same kind of dispersion relation is observed with a minimum value at π . However, the absolute value at $k = \pi$ is considerably smaller and scales like V^4 instead of V^2 . While the absolute value for $k = 0$ is only slightly smaller than the corresponding electronic gap, this is not the case for $k = \pi$ where the $U = 0$ relation (38) is completely changed. This can be attributed to the nesting of the Fermi surface in one dimension which leads to a near antiferromagnetic instability. Note that, although no long-range antiferromagnetic order exists at $T = 0$, nevertheless, antiferromagnetic correlations of the spins must be present because of the small energy for excitations at the zone boundary.

The dependence of the magnetic gap upon U in the Kondo-lattice regime, when $\epsilon_f = -U/2$, is shown in Fig. 4 where G_0^{mag} and G_π^{mag} have been plotted as a function of U for $N = 4, \varphi = 0$. For small U it seems that the gaps behave linearly with U or with a very strong U^2 term, considerably larger than for the electronic gap. It would be interesting to check this point by perturbation expansions in U . When $U \rightarrow \infty$, G_0^{mag} behaves as V^2/U , as do the electronic gaps, while the smallest gap G_π^{mag} tends to zero more quickly as V^4/U^2t . The same kind of differences between the order of magnitudes of the smallest electronic and magnetic gaps has been already observed on the Kondo-lattice Hamiltonian, where the electronic gap is of first order in J while the magnetic gap is of second order.²⁸ In the same manner as for the electronic gap, we have compared our results with the RG calcula-

tions⁷ done with blocks of three sites, represented by the dashed curve in Fig. 4. It is clear that the two results are very similar.

C. Mixed-valence regime

The corresponding results in the mixed-valence regime are presented in Figs. 6 and 11, and the dispersion in k has been reported in Fig. 8 to compare with the other regimes. Here also the magnetic gap for $k = \pi$ is an order of magnitude smaller than the $0 \rightarrow \pi$ minimum electronic gap. Nevertheless, even if the gap is very small, it tends to a constant value when $U \rightarrow \infty$. While the other gaps tend to values of order Δ , G_π^{mag} tends to a value which scales like $\Delta^2/t \sim V^4/t^3$. This is also a result of Fermi-surface nesting and indicates an incipient instability to antiferromagnetic order, as found in the Hartree-Fock calculations of the q -dependent susceptibility.³¹

V. DISCUSSION

The results presented above give exact descriptions of homogeneous mixed valence and the Kondo problem for small finite cells. The important problem is to extrapolate to the infinite one-dimensional lattice. In particular, it is essential to check whether the lowest electronic and magnetic gaps vanish or approach finite limits when $N \rightarrow \infty$. The comparison of our $N = 4$ results with calculations done on the infinite lattice, such as small- U perturbation expansion¹² or RG (Ref. 7) calculations for large U , is already a strong support. Also, the modified periodic boundary conditions help to extrapolate our results to $N \rightarrow \infty$. For example, we can com-

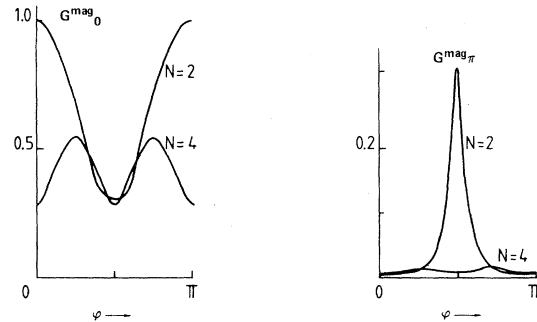


FIG. 11. Magnetic gaps G_0^{mag} and G_π^{mag} as a function of φ in the mixed-valence case for $\epsilon_f = 0$, $U = 1.5t$, $V = 0.2t$, and $N = 2$ and 4 .

pare $G_{\pi/2, \pi/2}^{\text{el}}$ for $N=2$ with antiperiodic boundary conditions ($\varphi=\pi$) with the same gap for $N=4$ with regular periodic boundary conditions ($\varphi=0$). By assuming a form $G=G^\infty+A/N$ leads definitively to $G^\infty \neq 0$. However, it would be necessary to reach larger cells to trust such a fit. In particular, much larger cells are required to approach the correct exponential form of the gap in the Kondo regime. The conclusions are more firm for the mixed-valence case. The fact that the gap is increased by the presence of U indicates that the gap remains in the limit $N \rightarrow \infty$ for this particular example of mixed valence.

There is another aspect that is extremely important in the extrapolation to $N=\infty$ —the symmetry of the lowest excitations. In our calculations the gap is always indirect, with the lowest excitation for electrons $\epsilon^+(k)$ at $k=0$ and for holes $\epsilon^-(k)$ at $k=\pm\pi$. By extrapolating this result to large N leads to two possibilities. If the gap $G_{0\pi}^{\text{el}}$ indeed remains positive as N is increased, then the true solution is an insulator. However, because $\epsilon^+(0)$ and $\epsilon^-(\pi)$ are at different points in the zone, i.e., they are excitations with different symmetry, it is allowed for the gap to go to zero and become negative. This would lead as $N \rightarrow \infty$ to a semimetallic solution with an electron Fermi surface around $k=0$ and a hole surface around $k=\pi$. Both possibilities are entirely consistent with the Luttinger conditions on the Fermi surface described for this case in Ref. 10. The important point is that the finding of the minimum energy excitations $\epsilon^+(0)$ and $\epsilon^-(\pi)$ at *different* points in k space is the proper expression of the Luttinger sum rule in the finite cell.

The parallel with the impurity case is very informative and is seen most clearly in the Kondo regime. As was discussed in Sec. III, for $V=0$ there is a simple d Fermi surface and a degenerate f state. However, for infinitesimal V , the degeneracy is lifted and there is a phase shift of $\pi/2$ of the states at the Fermi surface. This is caused by the well-known Kondo resonance and is fixed by the Friedel sum rule.³² In the lattice, for $V=0$ there is the same d Fermi surface and degeneracy of each f state. For any $V \neq 0$, there is also a Kondo-type resonance¹⁰ so that the Fermi surface is modified coherently at every site in accordance with the Luttinger sum rule.^{9,10} The present results show the consequences of the Kondo resonance in finite periodic cells in agreement with the sum rule, even though the magnitude of the gap is not representative of the $N \rightarrow \infty$ limit.

Some points are needed concerning the definition of the excitation energies and their physical meaning when $N \rightarrow \infty$. In particular, in a metallic situation, the lowest energies *always* vanish as $N \rightarrow \infty$ for all k . Thus the value for any given finite cell is not very useful. To give an example, let us consider a given band with an absolute minimum at $k=0$ which is partially filled by $2N+1$ electrons. Then the absolute ground state for $N_p=2N+1$ corresponds to $K=0$. Consider a shift of the momentum of each electron by $k/(2N+1)$; then we obtain the ground state in the subspace corresponding to $2N+1$ electrons subject to the condition that the total momentum is k . In the large-system limit the shift becomes infinitesimal and the change in energy vanishes, so that there is no dispersion of $E_{2N+1}(k)$. Thus, $\epsilon^\pm(k)$, as defined in (24), becomes meaningless in that case. However, there is one important case where this reasoning does not hold, and this is precisely the case that we consider here. This can be shown, for example, by the $U \sim 0$ case, where the band shape is given by Fig. 2. The ground state with $2N$ electrons corresponds to a completely filled subband. The extra electron is then added in another band and the extra momentum cannot be shared by the $2N$ other electrons because any shift of their momentum does not produce any resulting effect. In fact, $\epsilon^\pm(k)$ as defined above represent the true dispersion curves for electron and hole excitations as long as the gap remains for $N_p=2N$ even in the presence of electron-electron interactions.

It is also essential to consider extension to higher dimensions and to higher degeneracies in order to compare with experiments on anomalous rare-earth compounds. Such extensions would increase dramatically the present calculations. For example, exact solutions for small cells $\sim N=4$ would be very much more complex if we considered real d and f bands with as much as 10- and 14-fold degeneracies, crystal-field splittings, etc. These cases may potentially be treated by considering impurity problems³² and extending the results to periodic lattices using sum rules and symmetry requirements.¹⁰ For the present simple case with d and f bands having the same symmetry, all arguments suggest that the gap remains for all U . However, if there are bands of different symmetries at μ , or if the f state has internal structure, the gap in general disappears. In appropriate cases, the Luttinger conditions show that there *must* be a metallic Fermi surface and that, furthermore, in the Kondo and mixed-valence regimes, the quasiparticles at the Fermi surface must have interesting many-body enhancements.¹⁰

The tendency toward long-range magnetic order, of course, is an intrinsic property of an extended system. It remains a challenging problem to describe magnetic energies and excitations in more complex cases.

In conclusion, we have presented a method capable of giving exact results for a class of homogeneous mixed-valence and Kondo problems restricted to finite cells. Because of the difficulty of these problems there are many conflicting ideas in the literature,^{1,2} and it is very important to establish exact results to which approximate solutions are to be compared. The difficulty of the problem (even in the simplest Anderson Hamiltonian) forced us to consider at most cells with $N=4$ sites. In order to draw conclusions relevant to larger N , approaching $N \rightarrow \infty$, we have introduced modified boundary conditions (described in Sec. III) to allow better comparison of calculations with different N . Furthermore, we could use the symmetry of the periodic finite system to identify the important low-energy excitations, to follow them as N is changed, and to relate our results to general sum rules¹⁰ that fix the properties of the states near the Fermi energy for $N \rightarrow \infty$. In all cases where comparisons were possible, our $N=4$ results agreed well with $N=\infty$ calculations. Our concrete results are the electronic and magnetic gaps for the simplest Anderson-lattice Hamiltonian, Eq. (2) with two electrons per site, in all regimes (including small- U , Kondo, and mixed-valence). The important con-

clusions are the following: (1) There is a complete continuity among all regimes, each of which is found to have a nonmagnetic ground state. (2) The insulating gap is found in all regimes for this simplest Anderson-lattice Hamiltonian with two electrons per cell. In the mixed-valence regime the gap is *increased* by U giving strong support to the conjecture that the infinite system is indeed a nonmagnetic insulator for the Anderson lattice. (3) There is a tendency toward antiferromagnetic order that is very pronounced in our one-dimensional calculations, and which we believe is a result of the nesting of the Fermi surface. (4) There is a feature fixed at the Fermi surface which we termed the Kondo resonance, the width of which decreases with U in the Kondo regime. The exponential dependence typical of the Kondo problem is not found because it cannot be given by finite cells; however, the existence of the feature is established. (5) The results are in accordance with the sum-rule arguments^{9,10} on the nature of the Fermi surface in all regimes.

ACKNOWLEDGMENTS

We gratefully acknowledge many helpful interactions with our colleagues at Orsay and Xerox. We especially thank C. Herring, D. J. Chadi, and B. Brandow for their critical reading of the manuscript. One of us (R.M.M.) wishes to thank the National Science Foundation for travel support.

*Permanent address: Xerox Palo Alto Research Center, 3333 Coyote Hill Road, Palo Alto, CA 94304.

¹*Valence Instabilities and Related Narrow-Band Phenomena*, edited by R. D. Parks (Plenum, New York, 1977).

²*Valence Fluctuations in Solids*, edited by L. M. Falicov, W. Hanke, and M. P. Maple (North-Holland, Amsterdam, 1981).

³F. D. M. Haldane, *Phys. Rev. B* **15**, 2477 (1977).

⁴D. M. Newns and A. C. Hewson, *J. Phys. F* **10**, 2429 (1980).

⁵A. Bringer and H. Lustfeld, *Z. Phys. B* **28**, 213 (1977).

⁶T. V. Ramakrishnan, in *Valence Fluctuations in Solids*, Ref. 2, p. 13; T. V. Ramakrishnan and K. Sar, *Phys. Rev. B* **26**, 1798 (1982).

⁷R. Jullien, P. Pfeuty, A. K. Bhattacharjee, and B. Coqblin, *J. Appl. Phys.* **50**, 7555 (1979).

⁸C. Lacroix and M. Cyrot, *Phys. Rev. B* **20**, 1969 (1979).

⁹R. M. Martin and J. W. Allen, *J. Appl. Phys.* **50**, 7561 (1979); in *Valence Fluctuations in Solids*, Ref. 2, p. 85.

¹⁰R. M. Martin, *Phys. Rev. Lett.* **48**, 362 (1982); *J. Appl. Phys.* **53**, 2134 (1982).

¹¹H. J. Leder and B. Muhlschlegel, *Z. Phys. B* **29**, 347 (1978).

¹²K. Yamada and K. Yosida (unpublished).

¹³B. Brandow, *Int. J. Quantum Chem.* **13**, 423 (1979); in *Valence Fluctuations in Solids*; Ref. 2 p. 368.

¹⁴K. W. H. Stevens, *J. Phys. C* **11**, 985 (1978); **11**, L539 (1980), in *Valence Fluctuations in Solids*, Ref. 2, p. 79.

¹⁵See, for example, C. M. Varma and Y. Yafet, *Phys. Rev. B* **13**, 2950 (1976).

¹⁶M. Roberts and K. W. H. Stevens, *J. Phys. C* **13**, 5941 (1980); J. Geldenhuys, M. Roberts, and K. W. H. Stevens, *ibid.* **14**, 4279 (1982); A. J. Fedro and S. K. Sinha, in *Valence Fluctuations in Solids*, Ref. 2, p. 329.

¹⁷N. Grewe, H. J. Leder, and D. Entel, in *Festkorperprobleme (Advances in Solid State Physics)*, edited by J. Treush (Vieweg, Braunschweig, 1978), Vol. 20, p. 413, and references therein.

¹⁸R. G. Arnold and K. W. H. Stevens, *J. Phys. C* **12**, 5037 (1979).

¹⁹R. Jullien and R. M. Martin, *Solid State Commun.* **12**, 967 (1982); *ibid. J. Appl. Phys.* **53**, 2137 (1982).

- ²⁰P. W. Anderson, *Phys. Rev.* **124**, 41 (1961).
- ²¹K. G. Wilson, *Rev. Mod. Phys.* **47**, 773 (1975).
- ²²N. Andrei, *Phys. Rev. Lett.* **45**, 379 (1980); P. B. Vigman, *Zh. Eksp. Teor. Fiz. Pis'ma Red* **31**, 392 (1980) [*Sov. Phys.—JETP Lett.* **31**, 364 (1980)].
- ²³P. B. Vigman, *Phys. Lett.* **80A**, 163 (1980); N. Kawakami and A. Okiji, *Phys. Lett.* **86A**, 483 (1981).
- ²⁴J. R. Schrieffer and P. A. Wolff, *Phys. Rev.* **149**, 497 (1966).
- ²⁵L. C. Lopes, R. Jullien, A. K. Bhattacharjee, and B. Coqblin, *Phys. Rev. B* **26**, 2640 (1982).
- ²⁶R. Jullien, J. N. Fields, and S. Doniach, *Phys. Rev. B* **16**, 4889 (1977).
- ²⁷R. Jullien and P. Pfeuty, *J. Phys. F* **11**, 353 (1981).
- ²⁸R. Jullien, P. Pfeuty, and B. Coqblin, in *Valence Fluctuations in Solids*, Ref. 2, p. 169.
- ²⁹G. Spronken, R. Jullien, and M. Avignon, *Phys. Rev. B* **24**, 5356 (1981).
- ³⁰R. Whitehead, in *Theory and Application of Moment Method in Many Fermion Systems*, edited by J. B. Dalton, S. M. Grimes, J. P. Vary, and S. A. Williams (Plenum, New York, 1980).
- ³¹P. Riseborough and D. C. Mills, *Phys. Rev. B* **21**, 5338 (1980).
- ³²See, for example, P. Nozières and A. Blandin, *J. Phys. (Paris)* **41**, 193 (1980).